RSC Advances

PAPER

View Article Online
View Journal | View Issue

Cite this: *RSC Adv.*, 2017, **7**, 32637

Antimicrobials tethering on suture surface through a hydrogel: a novel strategy to combat postoperative wound infections†

Himadri Kalita,‡*[a] Ankita Hazarika,‡*[a] Sanjeeb Kalita,§[b] Raghuram Kandimalla§[b] and Rajlakshmi Devi *[a]

The present study aimed to develop a novel biocompatible suture biomaterial from Eri silk waste to avoid surgical site infections. To achieve this, silk waste fibers were reeled through a five-loop technique into a suture and embedded with an antimicrobial agents-growth factor cocktail in a hydrogel base comprising of Aloe-Vera and gum acacia (PRWSc). Characterization techniques like scanning electron microscopy (SEM), attenuated total reflection Fourier infrared spectroscopy (ATR-FTIR), thermo gravimetric analysis (TGA), and tensile properties analysis revealed the surface morphology, functionalization analysis, thermal and mechanical stability of PRWSc. Drug release study confirms the sustained release of the drugs from the suture. PRWSc was found to be biocompatible towards mammalian cells. *In vitro* antimicrobial study revealed that the PRWSc could inhibit the growth of Gram +ve, Gram −ve bacteria and opportunistic fungus. Further, confocal microscopy analysis confirmed the successful inhibition of biofilm on PRWSc surface. Clinical examination of the wound sutured with PRWSc revealed the successful wound healing which was confirmed by reduced microbial burden (CFU load) and inflammatory markers at the surgical site. This result was further confirmed by histopathology data where all skin adnexal structures were observed. This advanced suture material (PRWSc) can reduce the unwanted side effects of antibiotic overdose and can avoid serious problems related to postoperative complications.

Received 1st May 2017
Accepted 15th June 2017

DOI: 10.1039/c7ra04888b

rsc.li/rsc-advances

1. Introduction

Wound healing is a complex process that restores external and internal physical integrity of the body structure and involves several other complex interactions between the cells and other external environmental factors. The healing process starts as soon as the tissue injury occurs and it is categorized into four sequential and overlapping phases: homeostasis, inflammation, proliferation and remodelling.[1] These phases require perfectly coordinated cellular and molecular events involving several biological processes such as proliferation, differentiation, cell migration and increased biochemical activities. These biochemical events involve the components such as the extracellular matrix, cytokines, blood cells and growth factors. Growth factors are responsible for cell proliferation by the process of angiogenesis, myelogenesis, and gene transcription for accelerating the healing process.[1–3]

With the extensive use of sutures and other medical devices, the associated surgical site infections have been receiving greater attention. With an estimated 27 million surgical procedures each year, approximately 300 000–500 000 surgical site infections can be predicted to occur annually.[4] Infections associated with medical devices and sutures account for 44% of all of the nosocomial infections.[5] The consequence of surgical site infections includes longer hospital stays, extra financial costs, increased physiological and psychological burdens on patients and their families, and sometimes requiring an additional surgery to remove the infected implant.[6] One of the leading causes of infection at the wound site is the formation of biofilm on the surface of the surgical suture.[7] Incorporation of antimicrobial agents and growth factors on the suture biomaterial increases the rate of wound healing and prevents biofilm formation.[5] At the surgical site, infection due to bacteria like *Staphylococcus aureus*, *Staphylococcus epidermidis*, and opportunistic fungal pathogen like *Candida albicans* are more common.[8] So, using broad spectrum antimicrobial agents like amoxicillin, vancomycin, and amphotericin b can safely work against these microbial infections.

Natural non-absorbable biopolymer like silk fibroin is considered as promising biomaterial because of its desirable

[a]*Life Sciences Division, Institute of Advanced Study in Science and Technology (IASST), Paschim Boragaon, Garchuk, Guwahati-781035, Assam, India. E-mail: biochemistry.iasst@gmail.com; kalitahimadri123@gmail.com; ankitahazarikabiotech@gmail.com; Tel: +91-9706033567; +91-9706107073; +91-9706053605*

[b]*Drug Discovery Laboratory, IASST, Paschim Boragaon, Garchuk, Guwahati-781035, Assam, India*

† Electronic supplementary information (ESI) available. See DOI: 10.1039/c7ra04888b

‡ Himadri Kalita and Ankita Hazarika are co-first authors.

§ Sanjeeb Kalita and Raghuram Kandimalla are co-second authors.

characteristics. Silk fibroins are classified into two main types namely mulberry (*Bombyx mori*) and non-mulberry varieties including muga (*Antheraea assama*), eri (*Philosamia ricini*), tasar (*Antheraea mylitta*).[9] *Bombyx mori* silk fibroin (BMSF) has been characterised and commercially available biomaterial worldwide for centuries.[10] Among the non-mulberry silk *P. ricini* and *A. assama* has been widely studied in the field of biomaterial. The potential applicability of *P. ricini* waste fiber (PRWF) as suture biomaterial is yet to be fully explored. Although the utility of this waste material has been reported in the field of textile as conventional clothing material,[11] there is no scientific evaluation of the PRWF in the field of biomaterial till now. So in this present study, we have selected PRWF for the development of suture material. In this context, the present study was designed to develop a novel suture biomaterial to overcome all the drawbacks related to surgical site infections by impregnating the suture made from PRWF (PRWS) with broad spectrum antimicrobial agents (amoxicillin & amphotericin-b) and growth factors. A plant-based hydrogel system composed of gum acacia (GA) and Aloe-Vera (AV) has been used for efficient impregnation of drugs on the suture surface. Plant based gels and gum are reported to possess superior wound healing ability which accelerates the healing process. Hydrogel obtained from AV has an inherent ability to increase the collagen cross linking at wound site and accelerate the healing process. This is achieved by enhancing the wound contraction and breaking strength of the repaired tissue through escalation of the collagen type-III synthesis.[12,13] Natural gum, GA is composed of arabinogalactan, oligosaccharide, polysaccharides and is often used as a binding agent. This binding ability of GA can contribute to the efficient impregnation of antimicrobial agents on to the suture surface. GA also has antimicrobial activity, which can further contribute to faster tissue regeneration at the surgical site.[14] In view of this, it has been hypothesized in this study that the presence of this AV–GA hydrogel system can potentially serve the dual purpose of efficient drug loading on the suture surface and accelerate the wound healing cascade. The outcome of the study can fabricate a potential antimicrobial releasing suture biomaterial for prevention of postoperative wound infections.

2. Materials and methods

2.1. Materials

P. ricini (Eri) waste fiber was collected from Central silk Board, Guwahati, Assam, India. Processed fiber was sterilized by moist heat sterilization method in the autoclave (121 °C at 100 kPa pressure) for 20 min for further use. All the drugs and chemicals used in this study were procured from Sigma Aldrich, USA and Merck, Germany. Interleukin kites were procured from R&D systems, USA. BacLight bacterial viability kit was purchased from Life technologies, USA.

2.2. Methods

2.2.1. Preparation of suture from *P. ricini* silk waste. Suture was braided through five loop technique by reeling the fiber waste together (PRWS). Further, the braided suture was coated with a hydrogel containing antimicrobial agents and growth factors. Briefly-coating material was prepared by dissolving in 4.4% of antimicrobial agents (amoxicillin and amphotericin b, 9 : 1) and nerve growth factor (250 ng mL^{-1}) and epithelial growth factor (1 ng mL^{-1}) in a mixture of 0.1% hydrogel consist of AV and GA. Further PRWS was dipped in the coating solution and dried at 37 °C for 24 h (PRWSc).

2.2.2. Characterization of PRWS & PRWSc. The tensile properties of PRWS and PRWSc were measured with the tensiometer (Instron tensile tester 3343). Functional groups of both PRWS and PRWSc were determined by using attenuated total reflection-Fourier transform infrared spectra (ATR-FTIR) (NICOLET, Thermo Scientific, USA). Thermo gravimetric analysis (TGA) (Perkin Elmer TGA-4000, USA) for both the sutures PRWS and PRWSc was performed to determine the thermal stability. An internal standard commercial available BMSF suture was also kept for the above tests for better understanding. To determine the surface morphology both the sutures PRWS and PRWSc was observed under field emission scanning electron microscope (FESEM) (Carl Zeiss, SIGMAVP, Japan) and elemental analysis on the suture surface was determined by energy-dispersive X-ray spectroscopy (EDX) (INCA X-Max 250).

2.3. Biocompatibility evaluation

Before conducting *in vivo* analysis biocompatibility evaluation of blood contacting biomaterial is very much essential. In this study both the sutures PRWS and PRWSc were screened for biocompatibility towards mammalian cells by following experiments-

2.3.1. Cytocompatibility. Cytotoxicity of the PRWS and PRWSc were evaluated, and results were compared with commercially available BMSF suture. L929 cell line was obtained from National Centre for Cell Sciences (NCCS), Pune, India and maintained according to supplier guidelines. The cells were seeded on to 96 well plates (1×10^4 cells per well) and allowed to attach for 24 h. To determine the effect of the tested sutures on cells, the cells were treated with 10 mg of PRWS, PRWSc, and BMSF suture for 24, 48, 72 h by incubating at 37 °C in humidified CO_2 incubator. Cell viability was assessed using the spectrophotometry based MTT assay.[15] The percentage viability was calculated as the relative percentage of cells in the test sample with respect to cells in control sample.

$$\text{Viability (\%)} = \text{abs test/abs control} \times 100$$

2.3.2. Hemocompatibility. Hemocompatibility analysis of PRWS and PRWSc were performed and compared with BMSF suture. All the experiments were conducted in accordance with ICMR (Indian Council of Medical Research) guidelines for biomedical research on human participants. Experimental protocol was approved by human ethical committee, Institute of Advanced Study in Science and Technology, Guwahati, Assam, India. An informed consent was obtained from a human volunteer. Blood was collected in sterile vials containing

anticoagulant from the human volunteer, and the test is performed within 3 h after the collection suture materials (10 mg) were incubated for 1 h at 37 °C in the siliconized tube containing 10 mL of blood (diluted with saline in 1 : 9 ratio). After one hour tubes were centrifuged at 1500 rpm for 10 minutes. The absorbance of the supernatant was measured at 545 nm in a UV-visible spectrophotometer (Shimadzu, UV 1800, Japan).[16] The percentage of hemolysis was calculated by following formula-

$$\text{Hemolysis } (\%) = \frac{(\text{abs}_{\text{sample}} - \text{abs}_{\text{–ve control}})}{(\text{abs}_{\text{+ve control}} - \text{abs}_{\text{–ve control}})} \times 100$$

2.3.3. Effect on red blood cell (RBC) morphology. FESEM analysis of RBC was performed for evaluation of the morphology of RBC after incubation with suture materials. Briefly – after the incubation with suture materials from the above experiment the RBC pellet was collected and preceded for FE-SEM analysis. The RBCs from all the treatment groups were fixed in 3% glutaraldehyde for 4 h. Further cells were washed with 0.2 mM phosphate buffer saline (PBS) and incubated in same PBS for 6 h. After the incubation with PBS the cells were subjected to dehydration process by gradient acetone (30, 50, 70, 90, 95 & 100%) with 10 min incubation in each concentration and at last with dry acetone. Then the RBCs were incubated with tetra methyl silane for 15 min and evaporated to dryness until fine powder forms in a desiccator. Further, the RBCs from different treatment groups were observed for morphological changes under FE-SEM.

2.4. Evaluation of anti-thrombogenic property

The antithrombogenic properties of PRWS, PRWSc, and BMSF were evaluated using an *in vitro* kinetic method.[10] Citrate dextrose stabilized blood (2 mL) was incubated in micro centrifuge tubes for 1 h, each containing PRWS, PRWSc, and BMSF separately at 37 °C. After incubation, blood (0.2 mL) was taken from each tube and placed onto a clean sterilized glass plate. The glass plates were sterilized by autoclaving at high pressure saturated steam at 121 °C for around 15–20 min prior to perform the experiment. After the addition of 0.02 mL 0.1 M calcium chloride solution to the citrate dextrose treated blood, the clotting test was performed by the weight measurement of the amount of thrombus (clot) formed. The storage time of the blood was maintained at 30, 45 and 60 min. The blood clot was fixed in 5 mL formaldehyde solution (36% v/v) for 5 min after each particular time interval and further washed with distilled water, blotted with tissue paper and finally weighed the clot. The citrate dextrose treated blood without suture material was taken as control. The experiment is carried out in triplicate and repeated three times, and the result is reported as mean ± S.D.

2.5. Evaluation of *in vitro* antimicrobial activity

Antimicrobial property of the suture materials (PRWS & PRWSc) were examined by standard agar diffusion test and direct contact method. Further anti-biofilm property of the sutures was determined by confocal imaging of the suture through LIVE/DEAD Baclight bacterial viability assay kit.

2.5.1. Standard agar diffusion test method. Antimicrobial activity of PRWS and PRWSc were evaluated against *Staphylococcus aureus* (MTCC3160), *Escherichia coli* (MTCC40), and *Candida albicans* (MTCC3958) by using standard agar diffusion method.[17] Briefly, test bacterial and fungal cultures were grown on nutrient agar and sabouraud chloramphenicol agar plates respectively. The suture materials were placed on the agar plates and incubated at 37 °C for 24 h (bacteria) and 28 °C for 72 h (fungus). The clear zone around the suture was calculated using a scale and considered as the zone of inhibition. Market available BMSF suture was used as the control. The experiment is carried out in triplicate and repeated three times, and the result is reported as mean ± S.D.

2.5.2. Direct contact test method. BMSF, PRWS, and PRWSc were also evaluated for antimicrobial activity against Gram −ve (*E. coli*) and Gram +ve (*S. aureus*) through direct contact method. Initially, sutures were immerged in LB-medium containing bacterial culture at a concentration of 10^7 CFU mL^{-1} along with the density 60 μL cm^{-2}. This whole set up was incubated for 21 days at 37 °C. Further, the medium containing the bacteria was inoculated on nutrient agar medium and incubated at 37 °C for 24 h. Photographs were taken for each plate for verifying the microbial CFU. All the experiments were performed in triplicate for accuracy.[17,18]

2.5.3. Bacterial viability check (anti biofilm assay). After 21 days of incubation the sutures from the above experiment (BMSF, PRWS & PRWSc) were washed in PBS and stained with LIVE/DEAD® BacLight™ (Life Technologies, USA) for 30 min in dark condition. Further the sutures were observed under confocal microscope (Leica/TCS SP8, Germany).[19]

2.6. Drug release kinetics of PRWSc

The drug release profile of antimicrobial drugs and growth factors from the PRWSc suture was measured in PBS to study the drug release during usage. PRWSc (10 cm each) were placed in 1.5 mL centrifuge tube containing releasing medium (1.33 mL) of different pH (6.3, 6.6, and 7.7) which correspond to the different skin pH during healing and incubated at 37 °C with continuous shaking at 60 rpm. At different time points (24, 48, 72, 96, 120, and 144 h) 150 μL of each sample was withdrawn to measure the drug concentration and replaced with fresh media. The absorbance of the recovered aliquots were measured by using Multimode Reader, VARIOSKAN FLASH at different wavelengths 290 nm (pH 6.3), 289 nm (pH 6.6), and 287 nm (pH 7.7).[20]

2.7. *In vitro* degradation study

Enzymatic degradation study of the sutures was performed using a previously described method with slight modification.[21] Briefly, an enzyme solution was prepared by dissolving α-chymotrypsin Type I-S (Sigma, C7762) in Tris–HCL (pH-7.8). BMSF, PRWS, and PRWSc sutures were incubated in the enzyme solution at 37 °C for 14 days. After incubation period sutures were removed from the enzyme solution and dried

under vacuum at 50 °C. The weight of the dried sutures was measured and tensile strength evaluated. All the experiments were performed in triplicate and results were expressed in mean ± S.D.

2.8. Evaluation of healing ability of sutures on infected wounds

Male rats of Wister strain weighing 150–200 g was selected for the study and divided into three groups ($n = 6$). All the animals were housed at 25 ± 1 °C with a relative humidity of 45–55% and 12 : 12 h dark/light cycle. Animals were free to access water and standard pellet diet (Provimi, India) throughout the experimental period.[22] This study was performed in strict accordance with Committee for the Purpose of Control and Supervision of Experiments on Animals (CPCSEA) guidelines (registration number: 1706/GO/c/13/CPCSEA) and the protocol was approved by the Institutional Animal Ethical Committee of Institute of Advanced Study in Science and Technology, Guwahati-35, Assam, India (IASST/IAEC/2015-16/751).

2.8.1. Grouping

BMSF. Animals sutured with BMSF and infected with *S. aureus* (2×10^8 cells per mL) after 24 h of surgery.

PRWS. Animals were sutured with PRWS and infected with *S. aureus* (2×10^8 cells per mL) after 24 h of surgery.

PRWSc. Animals were sutured with PRWSc and infected with *S. aureus* (2×10^8 cells per mL) after 24 h of surgery.

2.8.2. Surgery protocol. Animals in all the groups were anesthetized with the ketamine (80 mg kg^{-1}) and xylasine (10 mg kg^{-1}) coke tail. Hair on the dorsal region was removed, and the area was cleaned with povidone iodine. The wound was created by making 25 mm full-thickness longitudinal incision with a scalpel. Further, wounded area was closed by making stitches with PRWS, PRWSc, and BMSF sutures and covered the wound with simple cotton gauze. After 24 h of surgery, the wounded area was infected with bacterial pathogen *S. aureus* (2×10^8 cells per mL). Post-surgery samples from the wound area and blood through retro-orbital route were collected on 3rd, 7th and 14th post-operative day to determine the bacterial load and inflammatory marker levels. At the end of 14 days all the animals were sacrificed and tissue specimens were collected from the incised wound and processed for histopathology analysis.

2.9. Determination of bacterial load/CFU count

At 3rd, 7th, and 14th post operative day tissue samples from the wounded area were excised, pulverized, and homogenized in sterile PBS. The resulting suspension was diluted and plated on nutrient agar and further incubated at 37 °C for 24 h. Results were normalized based on the tissue collected for determination of bacterial load.[8]

2.10. Measurement of inflammatory markers

Serum was separated by centrifuging the blood at 1500 rpm for 10 min and stored at −80 °C for further use. Inflammatory cytokines like (IL-1β & TNF-α) were estimated by using ELISA kits from R&D systems as per the instructions given by the manufacturer.

2.11. Histopathological analysis

Skin tissue from the surgical site was collected from all the groups and fixed in 10% buffered formaldehyde. Fixed samples were subjected to ethanol dehydration process (70, 90, and 100%) and embedded in the paraffin block. Sections of 5 μm thickness were made by using rotary microtome and stained with hematoxylin–eosin stain. The slides were examined under light microscope (LEICA EC3, Germany) for determination of pathological changes.[23–25]

3. Results

3.1. Characterization of suture material

3.1.1. Tensile strength. Being a manually braided suture PRWS did not show tensile strength as higher as that of the market available BMSF suture. However, tensile strength shown by PRWS was sufficient to be a potential suture biomaterial. Further coating with the binding agent on PRWS (PRWSc) surprisingly enhances the tensile strength, which might be due to fiber holding ability of the binding agent together. Table 1 showed the tensile properties of the PRWS, PRWSc, and BMSF. PRWSc showed 225 ± 20 g per den tenacity at maximum, where BMSF showed the tenacity of 290 ± 12 g per den.

3.1.2. Surface morphology. Suture surface under FESEM showed differences in the surface morphology of PRWS and PRWSc (Fig. 1A). The surface of the PRWS was found to be irregular, heterogeneous than that of PRWSc, which was smooth, homogeneous throughout the length. Further EDX analysis showed the presence of carbon (C) and oxygen (O) on the surface of PRWS and PRWSc, whereas additional element potassium (K) is present on the surface of PRWSc (ESI Fig. S1†).

3.1.3. TGA analysis. Thermal stability of PRWS, PRWSc, and BMSF was presented in the ESI Fig. S2.† The initial weight loss of the PRWS and PRWSc was observed at 94 °C. Further weight loss took place at temperature 250–300 °C, 350–400 °C, 550–600 °C. On the other hand, the BMSF showed the first phase of weight loss at 210 °C and the second phase of weight loss was evident around 350–400 °C. Results of this study indicate that BMSF was completely degraded at 400 °C whereas PRWS and PRWSc withstand up-to 600 °C.

3.1.4. Functional group analysis. ATR-FTIR spectra of PRWS and PRWSc are represented in Fig. 1B. In PRWS, the band at 1600–1700 cm^{-1} corresponds to amide I. Amide II position in PRWS appeared at 1500–1600 cm^{-1}. Also, band at 1200–1300 cm^{-1} corresponds to amide III and 1547 cm^{-1} corresponds to α helix of PRWS. Though amide I, II, and III were not predominant in PRWSc, the maximum amide I and amide II appeared at 1610 cm^{-1} and 1515 cm^{-1} respectively. Also ATR-FTIR of PRWSc showed major peaks at 656 cm^{-1} (O–H bending), 962 cm^{-1} (skeletal vibration, C–H bending), 1165 cm^{-1} (C–H and N–H bending), 1046 cm^{-1} (C–N bending), 1443 cm^{-1} (C–H bending, O–H bending, CH_2 ring bending, C–C ring stretching), 2361 cm^{-1} (C–N bending), and 2343 cm^{-1} (C–N bending).

Table 1 Tensile strength of BMSF, non-coated *P. ricini* waste suture (PRWS), and coated *P. ricini* waste suture (PRWSc)[a]

Sample	Maximum load (g)	Strain at maximum (%)	Young's modulus (g per den)	Tenacity at break (g per den)	Tenacity at maximum (g per den)	Toughness (g per den)
BMSF	2000 ± 170.05	43.97 ± 5.9	1453 ± 54.9	200 ± 12	290 ± 12	117 ± 7
PRWS	1998.49 ± 96	40.21 ± 5.28	1324 ± 115	178.75 ± 73	216.41 ± 16.04	110.48 ± 5.12
PRWSc	1990 ± 100	40.23 ± 3	1350 ± 50	180 ± 40	225 ± 20	115 ± 10

[a] All the results were expressed in mean ± S.D ($n = 3$).

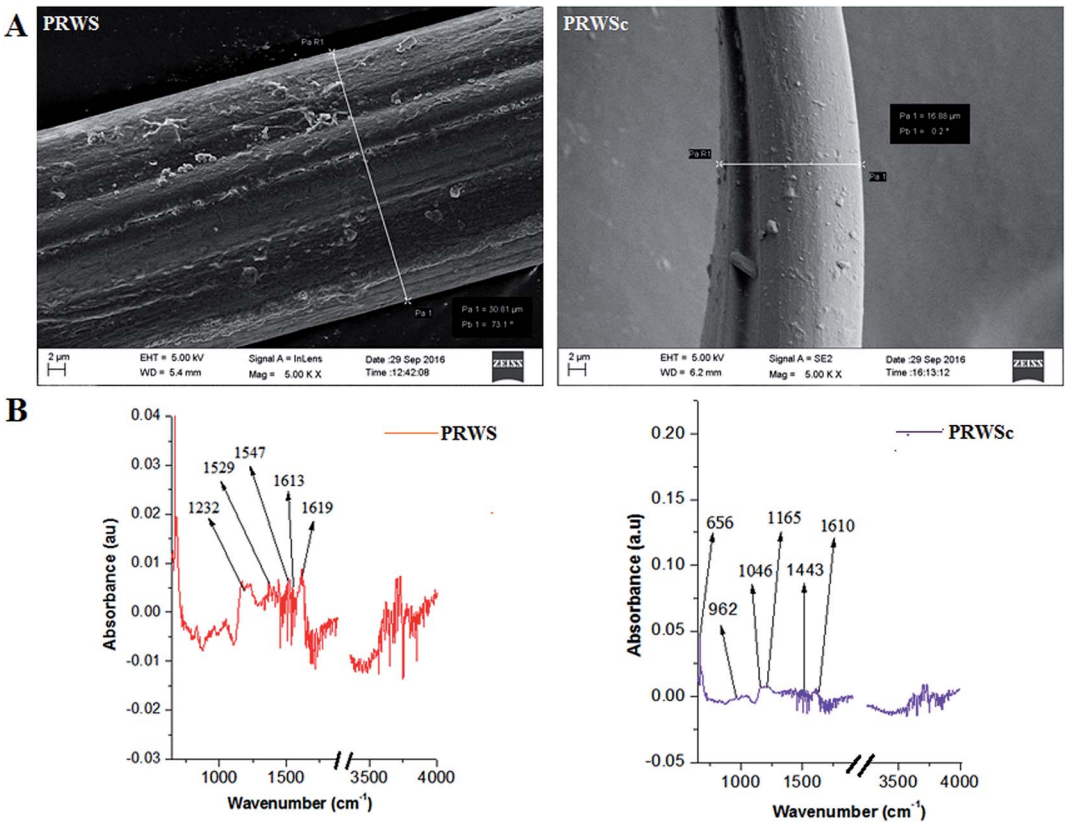

Fig. 1 Physico-chemical characterization of non-coated *P. ricini* waste suture (PRWS) and coated *P. ricini* waste suture (PRWSc) by using (A) field emission scanning electron microscope (FESEM) and (B) attenuated total reflection-Fourier transform infrared spectra (ATR-FTIR) analysis. For FTIR analysis spectral range is 650–400 cm^{-1}.

3.2. Biocompatibility evaluation

3.2.1. Cytocompatibility. PRWS, PRWSc, and BMSF did not induced significant cytotoxicity in the mouse L929 fibroblast cells. After 24, 48, and 72 h of post incubation of L929 cells with PRWS, PRWSc, and BMSF showed the viability of 91%, 85%, and 92% respectively. 75% cell viability after incubation of biomaterials with mammalian cells were considered to be non-toxic where the results of this study declare the tested suture materials were non-toxic (ESI Fig. S3†).

3.2.2. Hemocompatibility. BMSF, PRWS, and PRWSc exhibited very mild hemolysis towards human RBC (Fig. 2F, ESI Fig. S4†). The permissible hemolysis limit for the blood containing biomaterial is 5%, whereas the BMSF, PRWS, and PRWSc exhibited 0.34, 0.39, and 0.84% of hemolysis respectively. Thus the results demonstrate that suture materials do not have hemolysis components on their surfaces. The FE-SEM analysis of the RBC from different treatment groups further supports the biocompatibility of tested sutures where no morphological changes were observed in the treatment groups (Fig. 2A–E).

3.3. *In vitro* antithrombogenic property

For evaluating the *in vitro* antithrombogenic property *in vitro* blood clotting test was performed (ESI Fig. S5†). Thrombus formation was observed before and after the clotting time of 30, 45, and 60 min for control (A), BMSF (B), PRWS (C), and PRWSc (D). Non coated and coated sutures did not show any significant difference in the blood clotting process at different time interval.

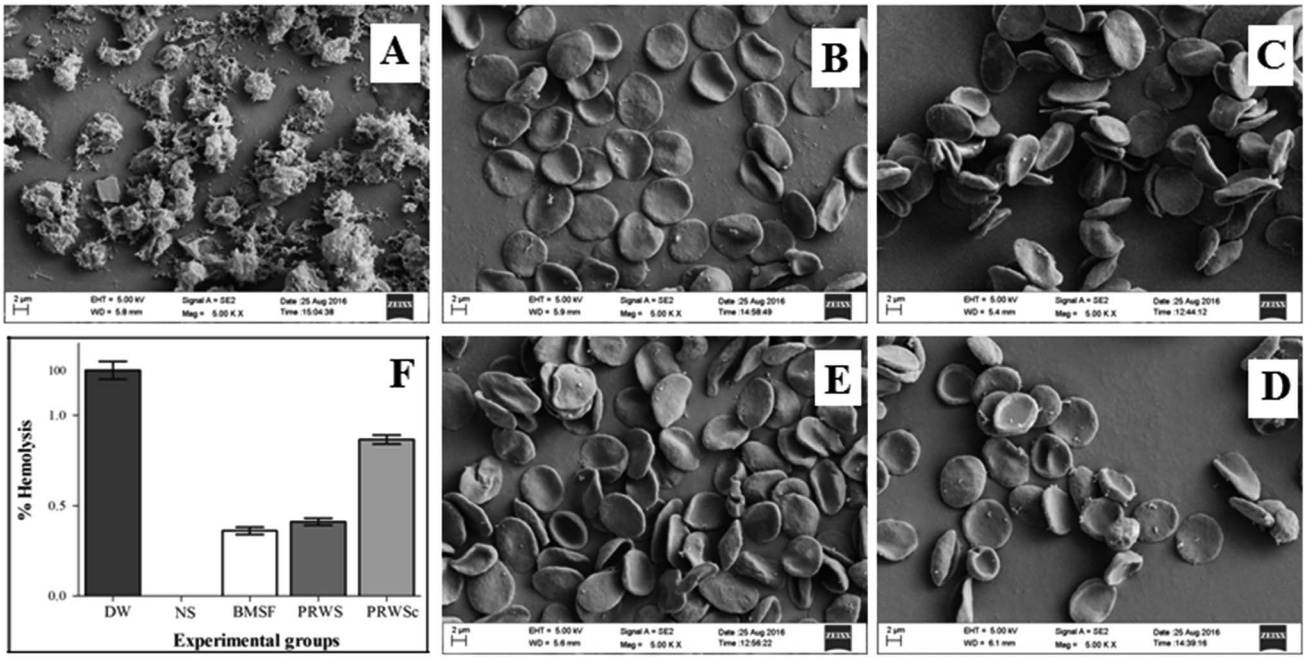

Fig. 2 Changes in the surface morphology of Red Blood Cell (RBC) in presence of different treatment (A) distilled water (DW), (B) normal saline (NS), (C) BMSF, (D) non coated *P. ricini* waste suture (PRWS), (E) coated *P. ricini* waste suture (PRWSc) under field emission scanning electron microscope. (F) Depicts the percentage of hemolysis in presence of DW, NS, BMSF, PRWS, and PRWSc.

3.4. Antimicrobial activity

3.4.1. Agar diffusion method. Antibacterial property of BMSF (a), PRWS (b), and PRWSc (c) in terms of zone of inhibition against Gram +ve (*S. aureus*) and Gram −ve (*E. coli*) bacteria were presented in Fig. 3A. BMSF and PRWS exhibit no antimicrobial activities against the tested strains of bacteria after 24 h of incubation. PRWSc showed a prominent zone of inhibition of 22 ± 3 and 33 ± 4 mm against *S. aureus* and *E. coli* respectively. PRWSc also inhibits the growth of opportunistic fungus *C. albicans* with a distinct zone of inhibition of 5 ± 0.3 mm, while PRWS and BMSF did not show considerable zone.

3.4.2. Direct contact test. To investigate the bacterial response to sutures *i.e.* BMSF (a), PRWS (b), and PRWSc (c), the media where these sutures were incubated for 21 days was re-

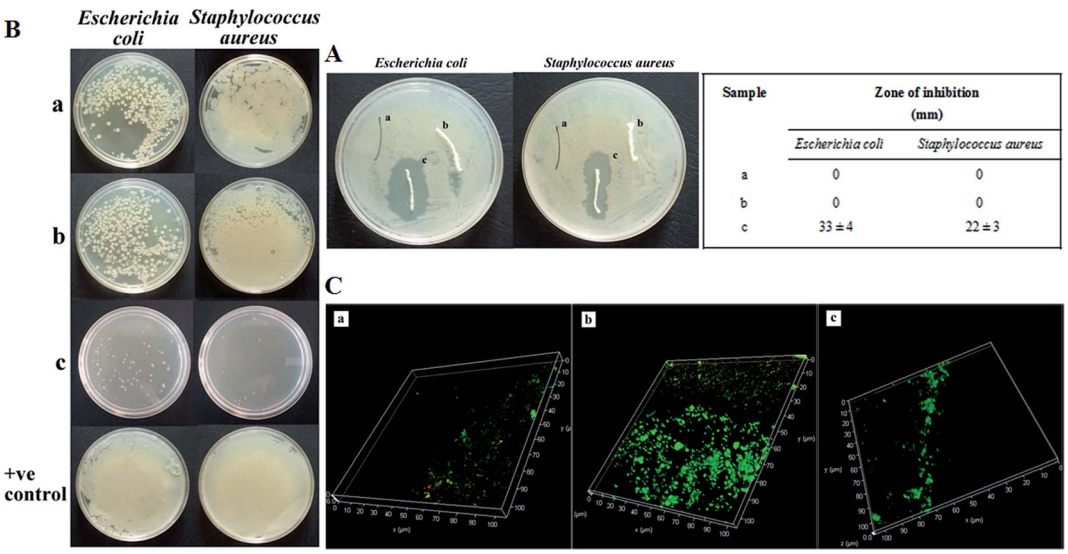

Fig. 3 Typical photograph showing antimicrobial activity of BMSF (a), non-coated *P. ricini* waste suture (PRWS) (b), and coated *P. ricini* waste suture (PRWSc) (c) against *Escherichia coli* and *Staphylococcus aureus*. (A) Standard agar diffusion test method, (B) re-cultured colonies of tested bacterial strain on agar plates, and (C) confocal microscopic examination showing viability of the bacteria (*S. aureus*) on the respective sutures, live bacteria appear green while dead ones are red. The seeded concentrations of bacteria on the sutures were 10^7 CFU mL^{-1}.

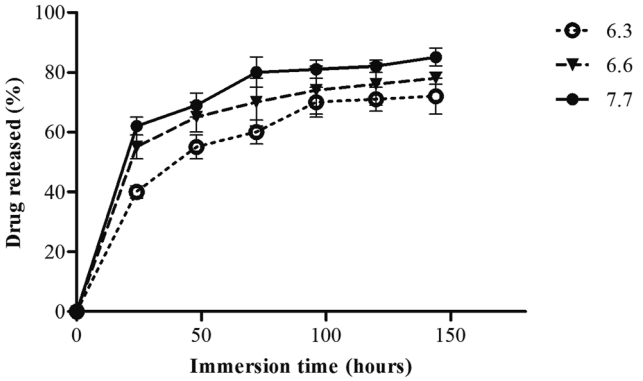

Fig. 4 *In vitro* amoxicillin release percentage from coated *P. ricini* waste suture (PRWSc) at three different pH 6.3, 6.6, and 7.7 up to 144 h.

cultured in agar. Fig. 3B showed the photographs of *E. coli* and *S. aureus* colonies on treatment with three tested sutures. As observed from the Fig. 3B it is clear that the tested bacteria cannot survive in the media incubated with PRWSc. While both PRWS and BMSF were not efficient to control the bacterial growth, since significant bacterial colonies were observed in post incubation.

3.4.3. Anti-biofilm assay. Confocal microscopy examination of the BMSF (a), PRWS (b), and PRWSc (c) incubated with *S. aureus* bacteria for 21 days showed adherence of bacteria (biofilm) on their surfaces (Fig. 3C). After incubation with bacteria, a large number of viable bacterial colonies (green colour) were observed on BMSF and PRWS surface. Whereas the bacteria found on the PRWSc was dead which attains red fluorescence.

3.5. Release kinetics of the drug from PRWSc

PRWSc demonstrated continuous drug release up to 5–6 days (Fig. 4). The initial burst of drug release was started at 24 h and remained stable after 96 h. The natural base material AV and GA facilitate continuous release of the antibacterial drug from the PRWSc at 72, 78, and 85% in various pH 6.3, 6.6, and 7.7 conditions. The results suggested that maximum drug release was observed in alkaline pH and lowest in acidic pH.

3.6. Degradation study

After 14 days of incubation period, changes were observed in terms of percentage loss in dry weight and tensile properties of the sutures. The non-coated suture (PRWS) showed a dry weight loss of 9 ± 1.32% and tensile strength loss of 7.01 ± 1%.

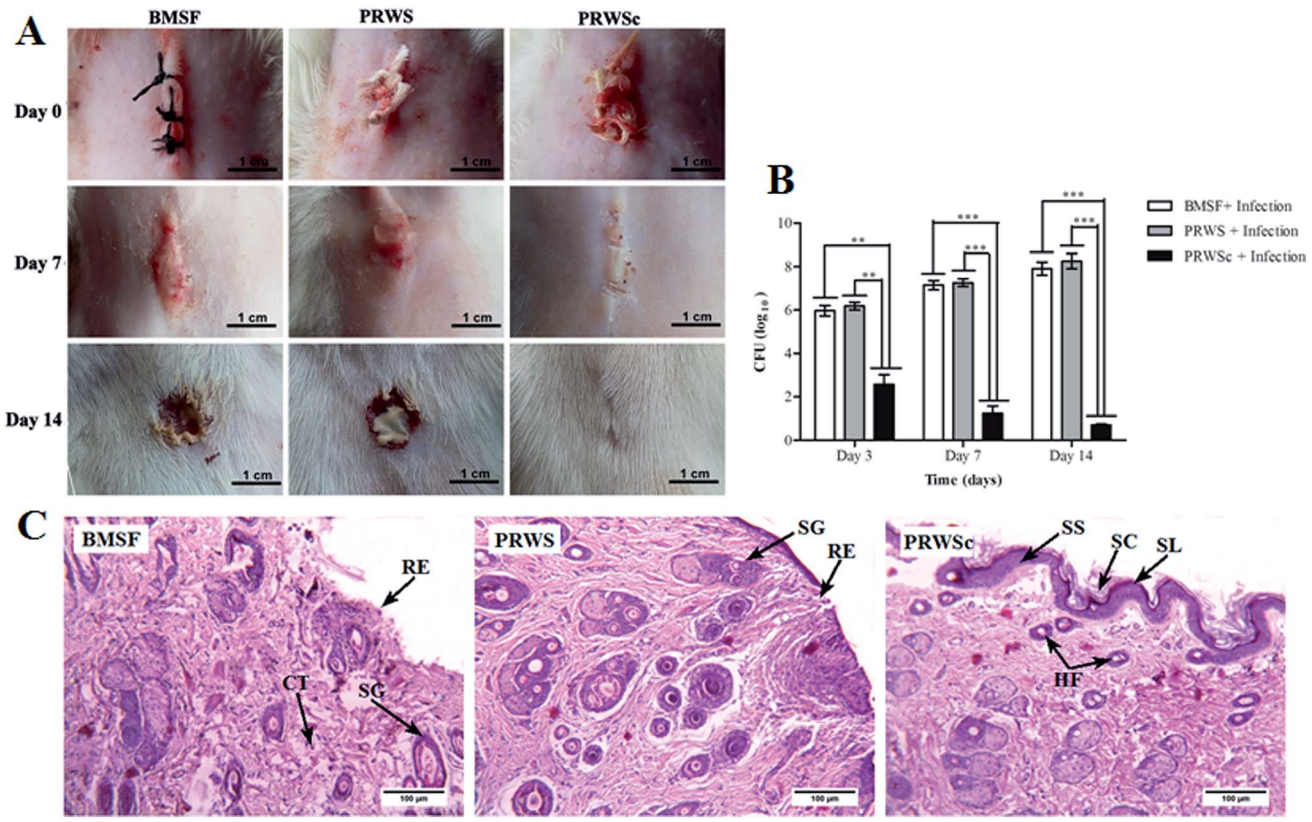

Fig. 5 (A) *S. aureus* (2×10^8 cells per mL) infected wound of animals sutured with BMSF, non-coated *P. ricini* waste suture (PRWS), and coated *P. ricini* waste suture (PRWSc) at 0^{th}, 7^{th}, and 14^{th} day. (B) Colony forming unit (CFU) count data of the *S. aureus* infected incised wound of BMSF, PRWS, and PRWSc stitched animal at 3^{rd}, 7^{th}, and 14^{th} post surgical day. (C) Histopathological changes of the skin tissue of animals sutured with BMSF, PRWS, and PRWSc on 14^{th} post-operative day showing ruptured epithelium (RE), sebaceous gland (SG) and collagen tissue (CT) in BMSF and BS stitched animal. Whereas re-epithelialisation of epidermis of BSc sutured animal with three distinct layer of skin namely stratum corneum (SC), stratum spinosum (SS), and stratum lucidum (SL), and reappearance of hair follicles (HR) were observed.

However, the hydrogel coated suture (PRWSc) demonstrated 10.99 ± 2% and 7.32 ± 1.2% loss of dry weight and tensile strength respectively. All the comparisons were made with commercial suture (BMSF) which exhibited 8.2 ± 1% loss in dry weight and 6.5 ± 1.1% loss in tensile strength (ESI Table S1†).

3.7. Wound healing assessment

3.7.1. Effect of PRWS and PRWSc on wound healing. The different phases of wound healing activities of *S. aureus* infected animal sutured with PRWS, PRWSc and BMSF at 0^{th}, 7^{th}, and 14^{th} day of the experiment are presented in Fig. 5A. Clinical examination of BMSF and PRWS sutured group of animal showed inflammation and bacterial infection from 3^{rd} post-operative day. However on day 7, animal sutured with PRWSc showed that there was no inflammation or bacterial infection at the repair site. In case of BMSF and PRWS sutured groups the incised wounds were severely infected and no sign of healing was observed at 14^{th} day. On the other hand, PRWSc sutured animals showed complete wound healing on day 14 with prominent hair growth at the wound site with no inflammation.

Wound healing is well supported by CFU count with a significant reduction in viable *S. aureus* in the wound area of the animal sutured with PRWSc. Significant increase in bacterial colonization (CFU) was observed in animals sutured with PRWS and BMSF at 3^{rd}, 7^{th}, and 14^{th} day of post operation. On the contrary, CFU count decreased surprisingly in PRWSc sutured animal, which indicates that *S. aureus* count was reduced significantly for the PRWSc sutured wound as compared to PRWS and BMSF (Fig. 5B).

3.7.2. Inflammatory response. Animal surgery with BMSF, PRWS, and PRWSc showed a significant increase in the levels of serum IL-1β (A) and TNF-α (B) compared to normal animals after 3^{rd} day (ESI Fig. S6†). Similar enhancement in the levels of these inflammatory makers was found on 7^{th} day of post-surgery in BMSF and PRWS sutured animal. On the contrary these levels were reduced in PRWSc sutured animal. On the 14^{th} day of post-operative surgery, IL-1β and TNF-α for BMSF and PRWS sutured animal reached the peak level as compared to control animal, whereas these levels were reduced in the case of PRWSc sutured animal.

3.7.3. Histopathological changes. Typical histological images of skin tissue collected from the incised area of BMSF, PRWS, and PRWSc sutured animals on 14^{th} post-operative day are shown in Fig. 5C. The wounded skin tissue sutured with BMSF and PRWS revealed the ruptured epithelium with distorted collagen and disappearance of hair follicles. Whereas, the wound sutured with PRWSc showed rapid disappearance of the inflammatory sign, reappearance of epidermis followed by sub-epidermal tissue namely stratum spinosum, stratum corneum, and stratum lucidum and hair follicles indicating complete tissue regeneration.

4. Discussion

Recent understanding of tissue remodeling and wound healing processes enable the researchers to contribute towards the development of cost effective wound management products.[26] Surgical suture mediated infections poses major concern during post-operative period that further lead to delayed wound healing and prolonged hospital stay. Antimicrobial drug releasing sutures avert biofilm formation and subsequent deeper tissue colonization of bacteria which can potentially reduce the complications of surgical site infection.[27]

Till date, to the best of our knowledge, no such suture material is available in the market which possesses the characteristics of an ideal suture like tissue compatibility, thermal stability, and superior tensile strength. In this context, the present proposition was made for the development of an antimicrobial drugs releasing suture having the ideal suture characteristics. Biomaterials from *B. mori*, *A. assama*, and *P. ricini* are already reported, however the silk from these mulberry and non-mulberry silkworms are mainly used in the textile industry.[28] Among these silk fibers, *P. ricini* is the cheapest and easy to rear without any environmental hazards.[29] During the reeling of the silk from the cocoon, tons of fibrous waste materials are generated every year.[30] The utility of this fibrous waste is yet to be realized for value-added purposes like fabrication of cost effective suture. In this study, fibrous waste of *P. ricini* was exploited for the development of a novel antimicrobial suture biomaterial. Tensile strength is the most crucial and primary requisite in the development of a suture material to reduce the possibility of breakage during the time of surgery.[31] Previous study reported that the greater percentage of C–H, C–C, and C–N unit at the surface of the fiber contribute to its tensile strength.[32] Hence the increased percentage of C and H on PRWSc might have resulted in its higher tensile strength.

Also, antimicrobial drug amoxicillin revealed the presence of characteristic peak for O13–H, C–H, N–H, C16–H, O25–H, CH_2 bending and C16–NH_2, C–C ring 2 stretching.[33] The detection of these functional groups on the PRWSc suture depicts the successful impregnation of amoxicillin on the suture surface. This have further lead to the prominent inhibition of infection in the surgical site sutured with PRWSc. Study reveals that aliphatic amine (C–N bending) and O–H bending are the markers of AV and GA.[34,35] Detection of these groups confirmed the presence of AV–GA based hydrogel system on the PRWSc suture surface. Inorganic mineral, potassium (K) is a component of AV hydrogel, which is essential for different enzymatic reactions modulating the wound healing process.[36] Thus, the identified K on PRWSc surface upon elemental analysis have come from the AV gel. Further TGA analysis of developed suture depicts that the suture biomaterial stable up to 600 °C. Interestingly the observed delay in thermal degradation of PRWS and PRWSc as compared to BMSF confirms that the fabricated suture is more thermally stable than BMSF.

The presence of broad spectrum antibiotic amoxicillin inhibits the growth of *S. aureus*.[37] This could be the reason for the prominent zone of inhibition exhibited by PRWSc against pathogenic *S. aureus*. The inhibited growth of *S. aureus* might have led to the prevention of biofilm formation on the suture surface as observed upon confocal analysis of PRWSc (Fig. 3C). The antifungal agent, amphotericin b is reported to inhibit the growth of opportunistic fungal pathogen *C. albicans*.[38] The

observed zone of inhibition against *C. albicans* in this could be attributed to the efficient coating of amphotericin b on the suture surface. This might have further contributed to the prevention of SSI and faster wound healing as observed *in vivo* analysis of PRWSc. A sustained drug release profile is necessary for prolonged antimicrobial activity and faster healing process.[17] Biomaterials prepared by AV gel blended with cellulose, chitosan, and gelatine is reported to exhibit anti-inflammatory and antibacterial properties.[39] This is due to the presence of polymers like galactan, glucomannan, and polysaccharide in AV.[39] The presence of this polymeric matrix contributes to the release of the drug from the AV-drug amalgam by leaching process further leading to its diffusion into the wound area, following a biphasic release mechanism.[40] GA acts as a natural binding agent, which possesses antimicrobial activity and finds wide use in therapeutic applications like wound dressing materials.[41] Thus, the biphasic drug release profile of PRWSc observed in this study is due to the presence of AV–GA hydrogel base. This might have also contributed to the faster wound healing of the surgical wound sutured with PRWSc by inhibiting microbial colonization on the sutures surface. It is important to analyze the *in vitro* biocompatibility and cytocompatibility of the suture biomaterials prior to *in vivo* application.[16] Studies have reported that the permissible limit of hemolysis of blood exposed to biomaterials is 5%.[16] In this study percentage hemolysis of PRWSc is below this permissible limit, which confirms its biocompatibility as a suture material. Hence it can be predicted that PRWSc would not show any adverse effects on human erythrocytes and this supports the possible coexistence of the fabricated suture in the human body without toxicity.

Growth factors in the wound site leads to tissue remodelling by enhancing the collagen synthesis which further induces the wound healing process.[42] Collagen plays an important role in the synthesis of connective tissue, which provides a framework in the regeneration of tissue in the healing area.[43,44] The prominent improvements in the ultrastructure of skin tissue stitched with PRWSc might have resulted due to the presence of growth factors in the coating material. Studies also reported that AV hydrogel contributes to the synthesis of collagen in wound site. This is rendered by the presence of muco-polysaccharide and acemannan in the hydrogel.[40] In this view, it can be predicted that the presence of AV and growth factors led to the formation of dense connective tissue in the PRWSc sutured wound site which resulted in its faster healing. AV has anti-inflammatory activity due to the presence of brady kinase enzyme, which helps to reduce excessive inflammation upon topical application on skin. This helps in stimulating immune defence system at the wound site and fasted the healing process.[45] The observed reduction in the level of inflammatory markers, TNF-α and IL-1β in the PRWSc sutured rats could be due to the anti-inflammatory activity of AV hydrogel. Reduction of these inflammatory marker levels in PRWSc sutured animal can be correlated with the accelerated wound healing process and thus support the present findings.

5. Conclusion

In this study we have prepared novel antimicrobial and growth factor impregnated suture, PRWSc from *P. ricini* (Eri) silk waste fiber using AV–GA hydrogel system. The prepared suture showed antimicrobial efficacy against *S. aureus*, *E. coli*, and *C. albicans* and could effectively prevent bacterial adherence on it. Slow and sustained release of drug was realized by diffusion of drug in aqueous medium, which was facilitated by the hydrogel. The hydrogel system also possesses inherent wound healing, anti-scar, antimicrobial properties which are helpful in fastening the healing process. Further, PRWSc prevents the surgical site infections and accelerates the wound healing process. This invention can outrage the applications of *P. ricini* silk waste fiber and introduces a novel strategy to combat surgical site infections for better healing of surgical wounds.

Author contributions

All authors made a significant contribution to the study and are in agreement with the content of the manuscript. Himadri Kalita and Ankita Hazarika conceived and designed the experiment, performed the experiments and analyzed the data and jointly wrote the paper as well and thus made an equal contribution to this study. Sanjeeb Kalita and Raghuram Kandimalla helped in conceiving the experiment and also in critical revision of the manuscript for important intellectual content. The final approval of the manuscript was done by Rajlakshmi Devi.

Conflict of interest

A portion of this work was used to file an Indian patent application (201631039604) dated 22nd November 2016.

Acknowledgements

The authors acknowledge Department of Science and Technology, Government of India, New Delhi, for financial support. We also acknowledge Institute of Advanced Study in Science and Technology (IASST), Guwahati, Assam, for providing necessary facilities. The authors acknowledge Central Silk Board, Assam, India for providing the Eri silk waste material. The authors thank Subrata Goswami, technical assistant, IASST for evaluating mechanical properties; Bikash Sarma and Achyut Konwar, PhD scholar, IASST for sample analysis using FESEM and TGA respectively. All the authors are grateful to Dr Anupam Banerjee, Manager Application Support, Leica Microsystem and Dr Bula Choudhury, Senior Scientist, Guwahati Biotech Park for their immense help with confocal microscopy.

References

1 M. Sengupta, J. Sengupta, P. Banerjee, M. Ghosh and S. Paul, *Muller J. Med. Sci. Res.*, 2015, **6**, 27–30.
2 S. Werner and R. Grose, *Physiol. Rev.*, 2003, **83**, 835–870.

3 D. Roth, M. Piekarek, M. Paulsson, H. Christ, W. Bloch, T. Krieg, J. M. Davidson and S. A. Eming, *Am. J. Pathol.*, 2006, **168**, 670–684.
4 C. Mingmalairak, *Antimicrobial Sutures: New Strategy in Surgical Site Infections*, A. Mendez-Vilas, Formatex Research Center, Spain, 2011, pp. 313–323.
5 S. Guo and L. A. Dipietro, *J. Dent. Res.*, 2010, **89**, 219–229.
6 X. Liu, T. Lin, J. Fang, G. Yao, H. Zhao, M. Dodson and X. Wang, *J. Biomed. Mater. Res., Part A*, 2010, **94**, 499–508.
7 J. Meyle, *Periodontal Pract. Today*, 2006, **3**, 253–268.
8 S. Kalita, R. Kandimalla, B. Devi, B. Kalita, K. Kalita, M. Deka, A. Chandra Kataki, A. Sharma and J. Kotoky, *RSC Adv.*, 2017, **7**, 1749–1758.
9 D. Gogoi, A. J. Choudhury, J. Chutia, A. R. Pal, M. Khan, M. Choudhury, P. Pathak, G. Das and D. S. Patil, *Biopolymers*, 2014, **101**, 355–365.
10 A. Jyoti, D. Gogoi, R. Kandimalla, S. Kalita, Y. B. Chaudhari, M. R. Khan, J. Kotoky and J. Chutia, *Mater. Sci. Eng., C*, 2016, **60**, 475–484.
11 D. Gogoi, A. J. Choudhury, J. Chutia, A. R. Pal, N. N. Dass, D. Devi and D. S. Patil, *Appl. Surf. Sci.*, 2011, **258**, 126–135.
12 A. Surjushe, R. Vasani and D. G. Saple, *Indian J. Dermatol.*, 2008, **53**, 163–166.
13 S. K. Verma and S. M. M, *Inter. J Biol. Med. Res.*, 2011, **2**, 466–471.
14 P. M. Sivakumar, V. Prabhawathi, R. Neelakandan and M. Doble, *Biomater. Sci.*, 2014, **2**, 990–995.
15 R. Kandimalla, S. Dash, S. Kalita, B. Choudhury, S. Malampati, R. Devi, M. Ramanathan, N. C. Talukdar and J. Kotoky, *Front. Cell. Neurosci.*, 2017, DOI: 10.3389/fncel.2017.00073.
16 R. Kandimalla, S. Kalita, B. Choudhury, D. Devi, D. Kalita, K. Kalita, S. Dash and J. Kotoky, *Mater. Sci. Eng., C*, 2016, **62**, 816–822.
17 A. Konwar, S. Kalita, J. Kotoky and D. Chowdhury, *ACS Appl. Mater. Interfaces*, 2016, **8**, 20625–20634.
18 J. Li, G. Wang, H. Zhu, M. Zhang, X. Zheng, Z. Di, X. Liu and X. Wang, *Sci. Rep.*, 2014, DOI: 10.1038/srep04359.
19 G. Limbert, R. Bryan, R. Cotton, P. Young, L. Hall-stoodley, S. Kathju and P. Stoodley, *Acta Biomater.*, 2013, **9**, 6641–6652.
20 X. Chen, D. Hou, L. Wang, Q. Zhang, J. Zou and G. Sun, *ACS Appl. Mater. Interfaces*, 2015, **7**, 22394–22403.
21 T. Arai, G. Freddi, R. Innocenti and M. Tsukada, *J. Appl. Polym. Sci.*, 2004, **91**, 2383–2390.
22 A. Hazarika, H. Kalita, D. C. Boruah, M. C. Kalita and R. Devi, *Nutrition*, 2016, **32**, 1081–1091.
23 A. Hazarika, H. Kalita, M. Chandra, Kalita and R. Devi, *Nutrition*, 2017, **38**, 95–101.
24 H. Kalita, D. C. Boruah, M. Deori, A. Hazarika, R. Sarma, S. Kumari, R. Kandimalla, J. Kotoky and R. Devi, *Front. Pharmacol.*, 2016, DOI: 10.3389/fphar.2016.00102.
25 N. Bhardwaj, Y. P. Singh, D. Devi, R. Kandimalla, J. Kotoky and B. B. Mandal, *J. Mater. Chem. B*, 2016, **4**, 3670–3684.
26 C. Vepari and D. L. Kaplan, *Prog. Polym. Sci.*, 2007, **32**, 991–1007.
27 J. Pedro, C. Serrano, L. García-fern, M. Barbeck, S. Ghanaati, R. Unger, J. Kirkpatrick, E. Arzt, L. Funk and P. Tur, *Biomaterials*, 2015, **52**, 291–300.
28 B. Talukdar, M. Saikia, J. Handique and D. Devi, *Int. J. Pure Appl. Sci. Technol.*, 2011, **7**, 81–86.
29 S. Dutta, B. Talukdar, R. Bharali, R. Rajkhowa and D. Devi, *Biopolymers*, 2013, **99**, 326–333.
30 U. C. Javali, N. V. Padaki, B. Das and K. B. Malali, *Developments in the use of silk by-product and silk waste*, 2015, DOI: 10.1016/B978-1-78242-311-9.00013-6.
31 D. Wu, H. Cui, J. Zhu, X. Qin and T. Xie, *J. Mater. Chem. B*, 2016, **4**, 2606–2613.
32 K. Mai-ngam, K. Boonkitpattarakul and J. Jaipaew, *J. Biomater. Sci., Polym. Ed.*, 2011, **22**, 2001–2022.
33 A. Bebu, L. Szabó, N. Leopold, C. Berindean and L. David, *J. Mol. Struct.*, 2011, **993**, 52–56.
34 F. Bouaziz, M. Koubaa, F. Barba, S. Roohinejad and S. Chaabouni, *Antioxidants*, 2016, DOI: 10.3390/antiox5030026.
35 L. S. Kassama, *International Journal of Contemporary Medical Research*, 2015, **5**, 30–39.
36 A. Femenia, E. S. Sánchez, S. Simal and C. Rosselló, *Carbohydr. Polym.*, 1999, **39**, 109–117.
37 K. D. Mlynek, M. T. Callahan, A. V. Shimkevitch, J. T. Farmer, J. L. Endres, M. Marchand, K. W. Bayles, A. R. Horswill and J. B. Kaplan, *Antimicrob. Agents Chemother.*, 2016, **60**, 2639–2651.
38 H. Nailis, D. Vandenbosch, D. Deforce, H. J. Nelis and T. Coenye, *Res. Microbiol.*, 2010, **161**, 284–292.
39 S. S. Silva, M. B. Oliveira, J. F. Mano and R. L. Reis, *Carbohydr. Polym.*, 2014, **112**, 264–270.
40 M. Tummalapalli, M. Berthet, B. Verrier, B. L. Deopura, M. S. Alam and B. Gupta, *Int. J. Biol. Macromol.*, 2016, **82**, 104–113.
41 B. A. Aderibigbe, K. Varaprasad, E. R. Sadiku, S. S. Ray, X. Y. Mbianda, M. C. Fotsing, S. J. Owonubi and S. C. Agwuncha, *Int. J. Biol. Macromol.*, 2015, **73**, 115–123.
42 A. Paige, V. Giuseppe and A. Travaglia, *J. Inorg. Biochem.*, 2016, **161**, 1–8.
43 E. Carolina, D. João, D. Masi, A. Carlos, L. Campos, F. David, J. De Masi, M. Aurelio, S. Ratti, I. Shin, R. David and J. De Mais, *Braz. J. Otorhinolaryngol.*, 2016, **82**, 512–521.
44 D. Grande, T. Lee, D. Ph and O. Limpisvasti, *Arthrosc. J. Arthrosc. Relat. Surg.*, 2010, DOI: 10.1016/j.arthro.2010.02.025.
45 S. Choi and M. H. Chung, *Semin. Integr. Med.*, 2003, **1**, 53–62.